

Analysis of Magneto Rheological Fluid Damper with Various Piston Profiles

Md. Sadak Ali Khan, A.Suresh, N.Seetha Ramaiah

Abstract – Control of seismic, medical and automobile vibrations represents a vast area of research that is growing rapidly. Magneto rheological (MR) dampers are a new class of devices that match well with the requirements and constraints of applications, including the necessity of having very low power requirements. The performance of MR damper depends on its magnetic and hydraulic circuit design. In this paper a finite element model is used to examine and investigate the 2- D axi-symmetric MR damper. Nine different configurations of piston for MR damper are simulated in order to investigate how the profile of the piston affected the maximum pressure drop that the damper could provide. The piston velocity and the input current to the coil are varied to evaluate the resulting change in magnetic flux density (B) and pressure drop (AP). The simulation results of the different configuration of piston show that the performance of single coil with filleted piston ends was better than that of other configurations for the same magnitude of input current and piston velocity.

Index terms - Magneto-rheological (MR) fluid, MR damper, Magnetic flux density, magnetic field intensity.

I. INTRODUCTION

Magnetorheological (MR) fluids have been investigated by many scholars as their material properties can be modulated through an applied electro- magnetic field. Specially, they are capable of reversibly changing from a linear Newtonian fluid to a semi solid with in a fraction of the milli seconds and the yield strength of this semi-solid is controllable. The fluid causes the maximum yield stress of about 50 to 100kPa. The magnetic field dependent shear strength of MR fluid depends on several factors including the size, composition, volume fraction of the particles and the strength of the applied magnetic field. Systems that take advantage of MR fluids are potentially simpler and more reliable than conventional electromechanical devices. Sodeyama and Suzuki et.al [1] have developed and tested an MR damper which provided maximum damping force of 300kN. Maher Yahya Salloom and Samad [2] designed an MR valve for which simulation was carried out by magnetic finite element software (FEMMR).

Manuscript published on 30 December 2012.

* Correspondence Author (s)

Md. Sadak Ali Khan*, Associate professor, Dept of Mech. Engg., M.J.C.E.T., Road No: 3, Banajara Hills, Hyderabad-34

A.Suresh, Principal, Sreyas Institute of Engineering and Technology, Thatti Annaram (V), Bandlaguda, Hyderabad - 65

N.Seetha Ramaiah, Professor, Dept of Mech. Engg. , M.J.C.E.T., Road No:3, Banajara Hills, Hyderabad-34

© The Authors. Published by Blue Eyes Intelligence Engineering and Sciences Publication (BEIESP). This is an open access article under the CC-BY-NC-ND license <http://creativecommons.org/licenses/by-nc-nd/4.0/>

H.yoshioka, J.C. Ramallo et.al.[3]constructed and tested MR fluid based damper on a base isolated two-degree freedom building model subjected to simulated ground motion which is effective for both far- field and near- field earthquake excitations. Jansen and Dyke [4] evaluated the performance of number of semi active control algorithms that are used with multiple MR dampers. Spancer and Dyke et.al. [5] Proposed a new model to effectively use as semi-active control device for producing a controllable damping force portraying the nonlinear behavior of MR fluid damper. N.Seetaramaiah and Sadak et.al. [6] have designed a small capacity MR fluid damper which achieved the requirements of dynamic range and controllable force. Lai and W.H Liao [7] have found that MR fluids can be designed to be very effective vibration control actuators. Butz,T and Von Stryk [8] have given overview on the basic properties of electro and magnetorheological fluids and discussed various phenomenological models for devices . Laura M, Jansen and Shirley J. Dyke[9] presented the results of a study to evaluate the performance of a semi active control algorithms for use with MR dampers.Henri Gavin Jesse Hoagg et.al[10] have made a comparison between ER and MR devices in the context of electrical power requirements.

The present paper analyzes the force for vibration control by using nine different models of MR damper using ANSYS software. The main objective of the paper is to evaluate the nine different models of MR damper using ANSYS software.

II. NOMENCLATURE

A_p	:	piston cross section area
d	:	spool length
d_{cyl}, d_{sh}	:	diameters of the cylinder and shaft respectively
e	:	house thickness
H	:	fluid viscosity in the absence of the field, C
I	:	current
L, g, W	:	length, gap and width of the flow channel between the fixed poles
N	:	number of turns
Q	:	volumetric flow rate
V_p	:	velocity of the piston
τ	:	shear stress,
τ_y	:	field-dependent yield stress,
ΔP_η	:	viscous component of pressure drop
ΔP_τ	:	yield stress component of pressure drop
γ	:	Fluid shear rate

Analysis of Magneto Rheological Fluid Damper with Various Piston Profiles

- 1P : one stage coil with plain ends
- 1C : one stage coil with chamfered ends
- 1F : one stage coil with filleted ends
- 2P : two stage coil with plain ends
- 2C : two stage coil with chamfered ends
- 2F : two stage coil with filleted ends
- 3P : three stage coil with plain ends
- 3C : three stage coil with chamfered ends
- 3F : three stage coil with filleted ends
- MFD : Magnetic Flux density

III. THEORETICAL ANALYSIS

The damper design is done based on the following facts. The mechanical energy required for yielding increases with increase in applied magnetic field intensity which in turn increases yield shear stress. In the presence of magnetic field, the MR fluid follows Bingham's Plastic flow model, given by the equation

$$\tau = \eta \dot{\gamma} + \tau_y(H) \quad \tau > \tau_y$$

The above equation is used to design a device which works on the basis of MR fluid. The total pressure drop in the damper is evaluated by summing the viscous component and yield stress component, which is approximated as

$$\Delta P = \frac{12\eta QL}{g^3 W} + \frac{C\tau_y L}{g}, \quad \text{where}$$

$$\eta = 0.0006 \gamma^{-0.6091}$$

$$A_p = \frac{\pi [(d_{cyl} - 2g)^2 - d_{sh}^2]}{4}$$

$$Q = A_p V_p$$

$$W = \pi (d_{cyl} - g)$$

$$C = 2.07 + \frac{12Q\eta}{12Q\eta + 0.4Wg^2\tau_y}$$

the value of the parameter, C ranges from a minimum of 2 (for $\Delta P_{\tau} / \Delta P_{\eta}$ less than ~1) to a maximum of 3 (for $\Delta P_{\tau} / \Delta P_{\eta}$ greater than ~100).

In order to calculate the change in pressure on either side of the piston within the cylinder, yield stress is required which is obtained from the graph of yield stress vs magnetic field intensity provided by Lord corporation for M.R. fluid -132 DG.

IV. FINITE ELEMENT MODELING OF MR DAMPER

The MR damper consists of a copper coil which is wound on a piston. An annular gap of 0.4 mm is maintained between the piston and its housing. Mild steel is used for the piston due to its high relative permeability. The contribution current to the coil is ranging from 0.2A to 2A which is the diffusion current for the standard MR fluid 132 DG. This paper presents

analysis of a 2D axisymmetric MR damper for nine different configurations. In these models the proportions of the piston, number of turns of the coil and annular gap are kept constant while different shapes of piston with plain, chamfered and filleted ends are considered. The design proposed of the MR damper consists of a steel path and an annular gap as shown in Fig. 1. Further the piston is considered with one, two and three stages in order to maintain two, three and four poles respectively as shown in Fig. 2 to 10.

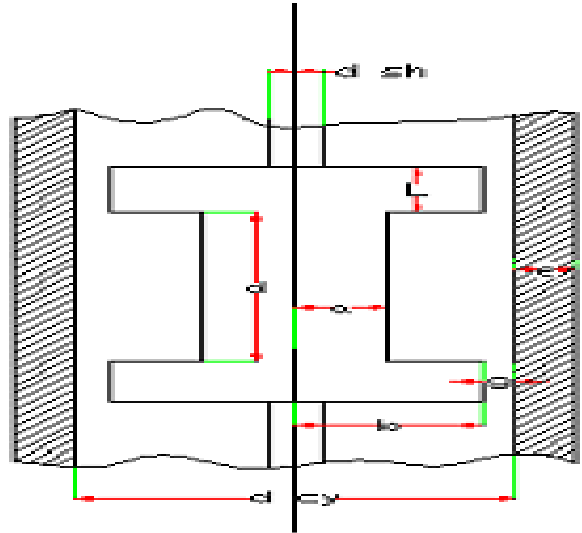


Fig.1 Schematic shows the design and dimensions of MR damper

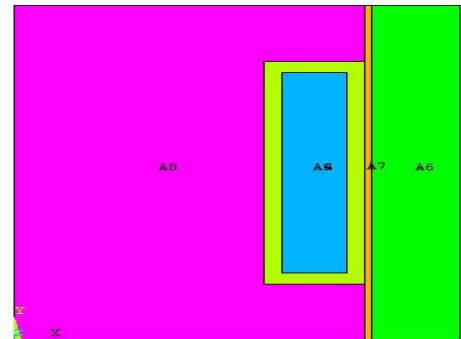


Fig.2. One stage coil with plain ends

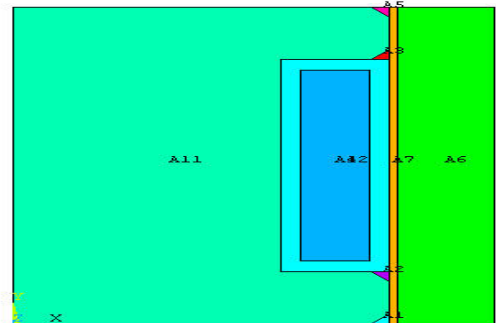


Fig.3. One stage coil with chamfered ends

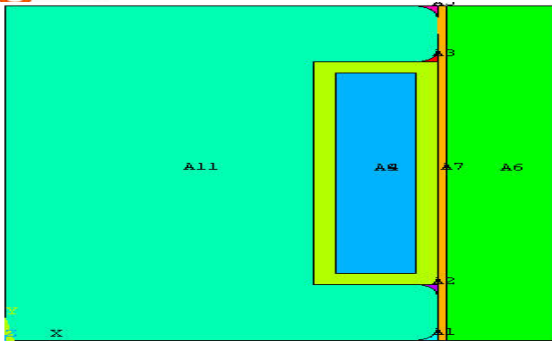


Fig 4. One stage coil with filleted ends

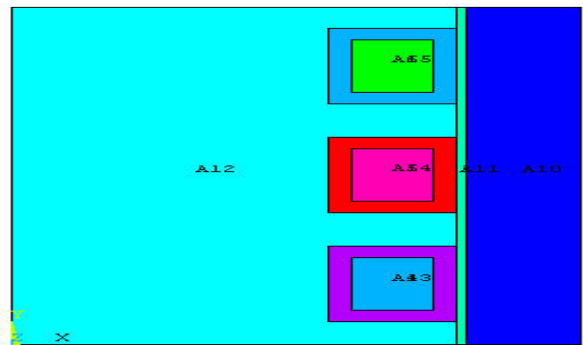


Fig 8. Three stage coil with plain ends

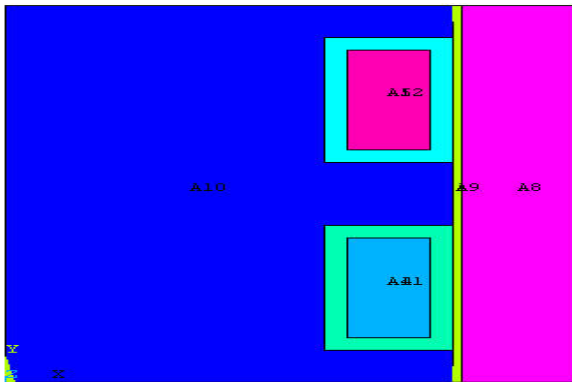


Fig 5. Two stage coil with plain ends

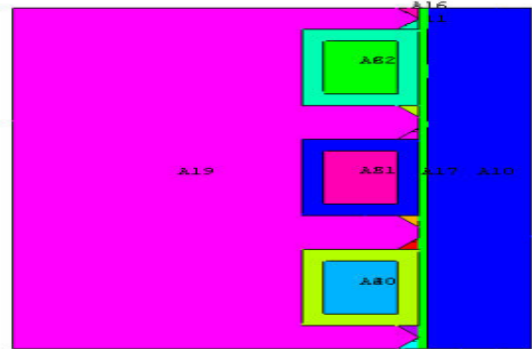


Fig 9. Three stage coil with chamfered ends

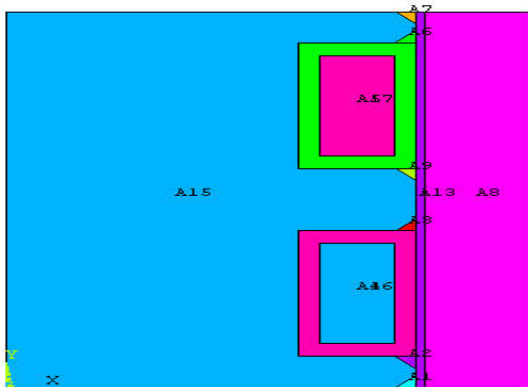


Fig 6. Two stage coil with chamfered ends

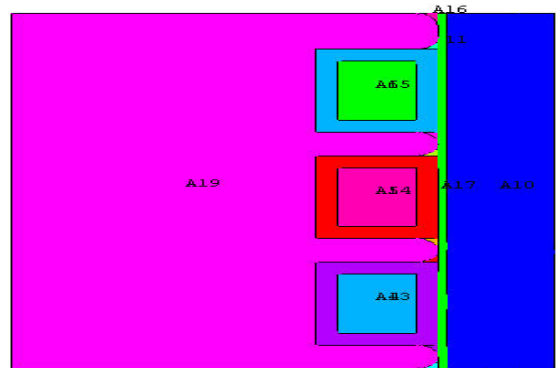


Fig 10. Three stage coil with filleted ends

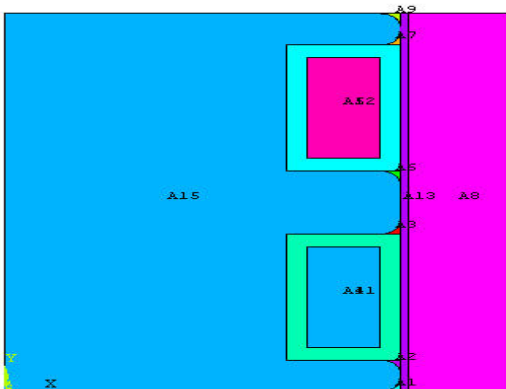


Fig 7. Two stage coil with filleted ends

These models are analyzed to study the variation of magnetic field intensity and magnetic flux density with respect to the input current to the coil. Analysis is carried out using ANSYS[®] 11 software. The variation of 2D flux lines, magnetic flux density and magnetic field intensity for the different models at a current of 2A are shown in Fig.11 to Fig.24

It can be observed from fig.11 and fig.13 that the flux lines are continuous loops in case of one and three coils. There are two separate loops in case of three coils model since it has even number of poles whereas in case of two coils model (Fig.12) the flux lines form a single loop due to odd number of poles. There is a concentration of flux lines near the MR fluid gap.

Analysis of Magneto Rheological Fluid Damper with Various Piston Profiles

Moreover, the flux lines shift their path when they reach the MR fluid gap, since the properties of MR fluid are different from that of piston and cylinder.

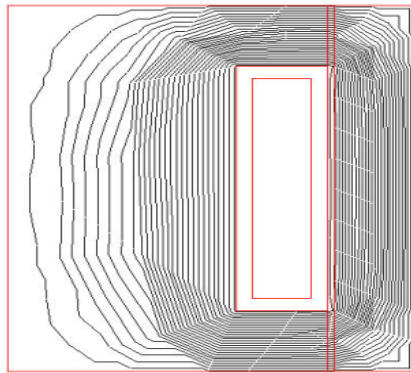


Fig 11. Flux lines around the one stage coil

```
ANSYS 11.0
MAY 5 2011
09:39:31
NODAL SOLUTION
STEP=2
SUB =1
TIME=2
AZ
RSYS=0
SMX =2.469
.045724
.137173
.228622
.41152
.502969
.594418
.777316
.868765
.960214
1.143
1.235
1.417
1.509
1.6
1.783
1.875
1.966
2.149
2.24
2.423
```

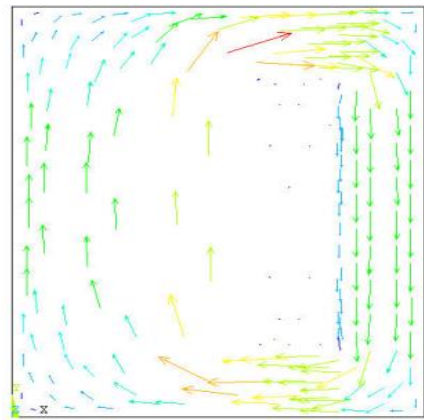


Fig 14 MFD vectors for one stage coil

```
ANSYS 11.0
MAY 5 2011
09:40:05
VECTOR
STEP=2
SUB =1
TIME=2
B
ELEM=173
MIN=.005069
MAX=4.275
.47951
.959951
1.428
1.903
2.377
2.852
3.326
3.801
4.275
```

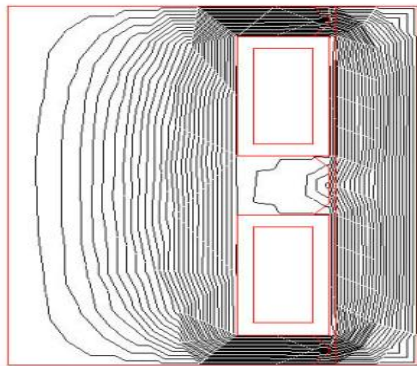


Fig 12. Flux lines around the two stage coil

```
ANSYS 11.0
MAR 25 2011
11:59:29
NODAL SOLUTION
STEP=2
SUB =1
TIME=2
AZ
RSYS=0
SMX =.683119
.01265
.037951
.063252
.088552
.139154
.164455
.189755
.240357
.256557
.290958
.34156
.36686
.392161
.417462
.468063
.493364
.518665
.569266
.594567
.619867
.670469
```

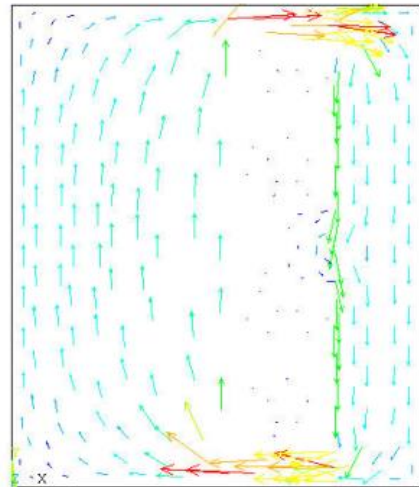


Fig 15. MFD vectors for two stage coil

```
ANSYS 11.0
MAR 25 2011
12:01:05
VECTOR
STEP=2
SUB =1
TIME=2
B
ELEM=235
MIN=.001358
MAX=1.933
.001358
.215981
.430605
.645228
.859852
1.074
1.289
1.504
1.718
1.933
```

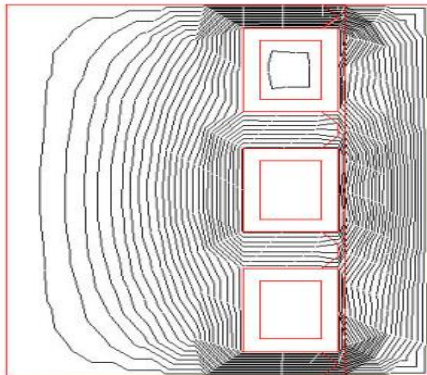


Fig 13. Flux lines around the three stage coil

```
ANSYS 11.0
MAR 25 2011
22:25:36
NODAL SOLUTION
STEP=2
SUB =1
TIME=2
AZ
RSYS=0
SMX =.550607
.010196
.030589
.050982
.071375
.112161
.132554
.152946
.193732
.214125
.234518
.275303
.295696
.316089
.336482
.377268
.397661
.418053
.458839
.479232
.499625
.54041
```

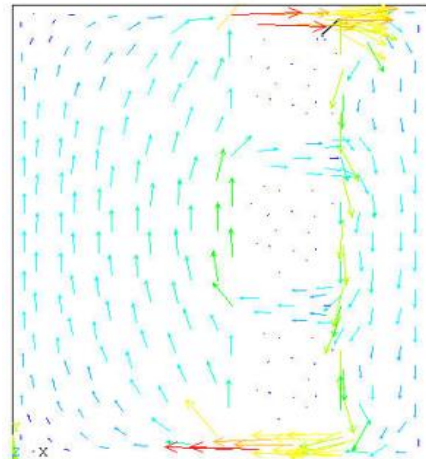


Fig 16. MFD vectors for three stage coil.

```
ANSYS 11.0
MAR 25 2011
22:25:58
VECTOR
STEP=2
SUB =1
TIME=2
B
ELEM=355
MIN=.812E-03
MAX=1.41
.812E-03
.157353
.313894
.470435
.626976
.783517
.940058
1.097
1.253
1.41
```

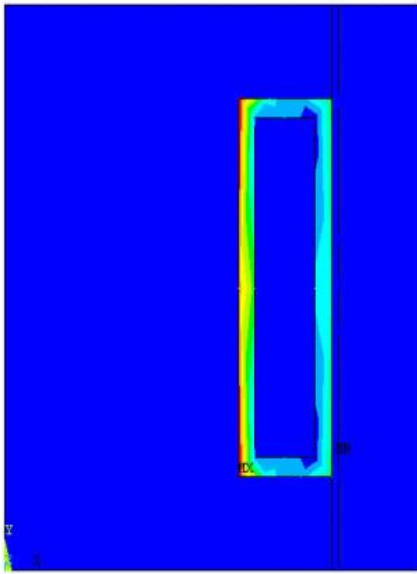



Fig 17. Magnetic field intensity for one stage coil

```
ANSYS 11.0
MAY 5 2011
09:40:59
NODAL SOLUTION
STEP=2
SUB =1
TIME=2
HSUM (AVG)
RSYS=0
PowerGraphics
EFACET=1
AVRES=Mat
SMN =1.117
SMX =.166E+08
1.117
.185E+07
.369E+07
.554E+07
.738E+07
.923E+07
.111E+08
.129E+08
.148E+08
.166E+08
```

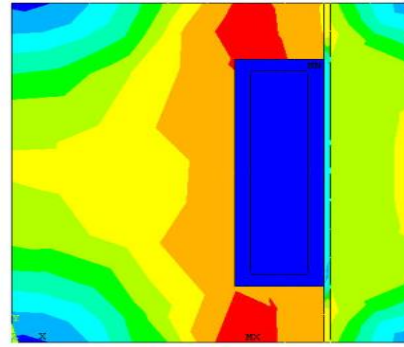


Fig 20. MFD vector sum for one stage coil

```
ANSYS 11.0
MAY 5 2011
09:43:11
NODAL SOLUTION
STEP=2
SUB =1
TIME=2
BSUM (AVG)
RSYS=0
PowerGraphics
EFACET=1
AVRES=Mat
SMN =.004297
SMX =3.297
.3702
.736103
1.102
1.468
1.834
2.2
2.566
2.932
3.297
```

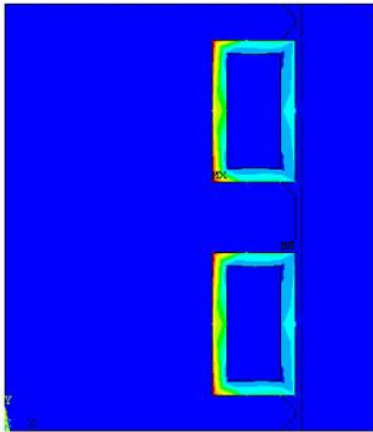


Fig 18. Magnetic field intensity for two stage coil

```
ANSYS 11.0
MAR 25 2011
12:02:16
NODAL SOLUTION
STEP=2
SUB =1
TIME=2
HSUM (AVG)
RSYS=0
PowerGraphics
EFACET=1
AVRES=Mat
SMN =.411129
SMX =.546E+07
.411129
.606512
.121E+07
.182E+07
.243E+07
.303E+07
.364E+07
.425E+07
.485E+07
.546E+07
```

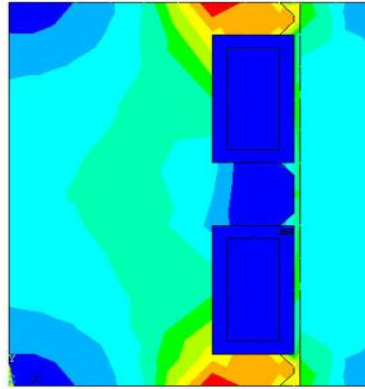


Fig 21. MFD vector sum for two stage coil

```
ANSYS 11.0
MAR 25 2011
12:02:42
NODAL SOLUTION
STEP=2
SUB =1
TIME=2
BSUM (AVG)
RSYS=0
PowerGraphics
EFACET=1
AVRES=Mat
SMN =.002186
SMX =1.929
.002186
.216302
.430418
.644534
.85865
1.073
1.287
1.501
1.715
1.929
```

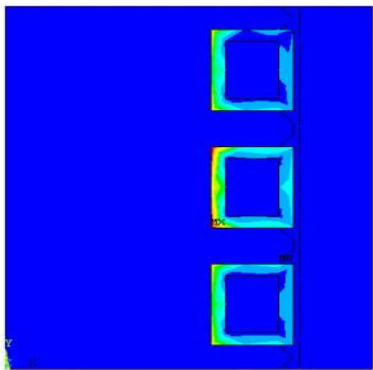


Fig 19. Magnetic field intensity for three stage coil

```
ANSYS 11.0
MAR 25 2011
22:26:49
NODAL SOLUTION
STEP=2
SUB =1
TIME=2
HSUM (AVG)
RSYS=0
PowerGraphics
EFACET=1
AVRES=Mat
SMN =.706864
SMX =.458E+07
.706864
.808613
.102E+07
.153E+07
.203E+07
.254E+07
.305E+07
.356E+07
.407E+07
.458E+07
```

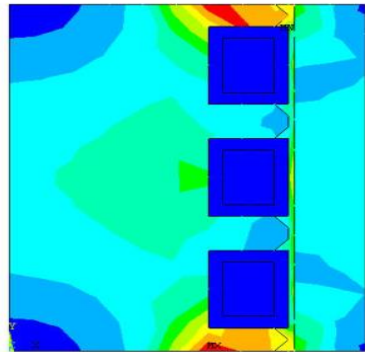


Fig 22. MFD vector sum for three stage coil

```
ANSYS 11.0
MAR 25 2011
22:27:15
NODAL SOLUTION
STEP=2
SUB =1
TIME=2
BSUM (AVG)
RSYS=0
PowerGraphics
EFACET=1
AVRES=Mat
SMN =.819E-03
SMX =1.384
.819E-03
.154496
.308173
.46185
.615527
.769204
.922881
1.077
1.23
1.384
```

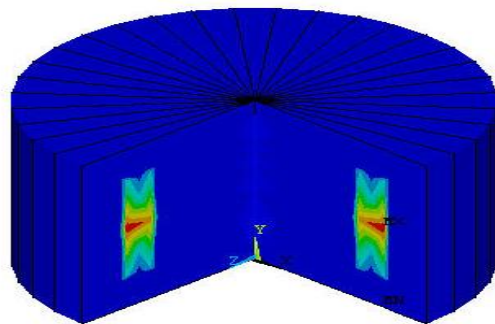


Fig 23. 3-D Axisymmetric view of MR fluid damper one stage coil

Analysis of Magneto Rheological Fluid Damper with Various Piston Profiles

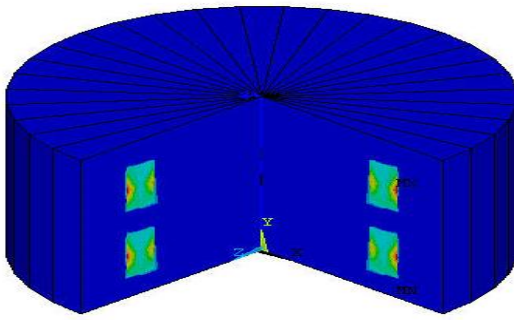


Fig 24. 3-D Axisymmetric view of MR fluid Damper two stage coil

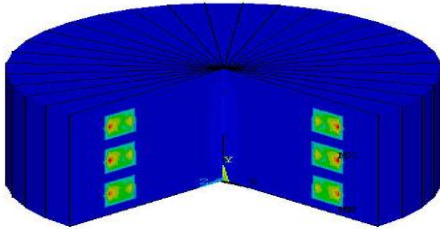


Fig 25. 3-D axisymmetric view of MR fluid Damper three stage coil

V. SIMULATION RESULTS AND ANALYSIS

The simulation results of pressure drop with respect to magnetic flux density for a variation in piston velocity from 0.04 m/s to 0.2 m/s and constant gap of 0.4 mm for various models are shown in Fig. 26a to Fig.26

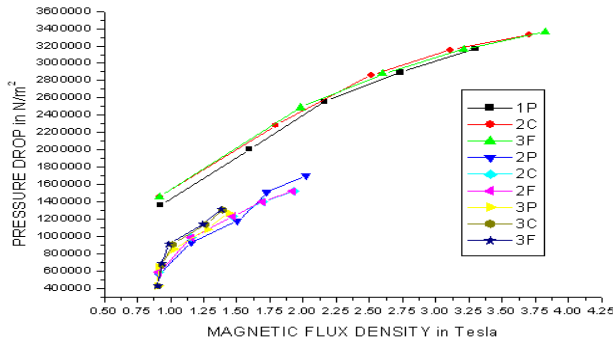


Fig 26 a. Variation of Pressure drop with Magnetic Flux Density for a Piston Velocity of 0.04 m/s

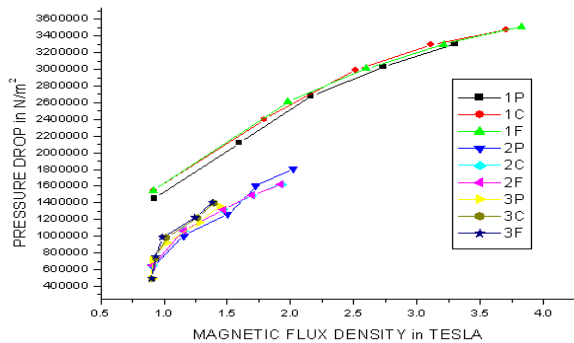


Fig 26 b. Variation of Pressure drop with Magnetic Flux Density for a Piston Velocity of 0.08 m/s

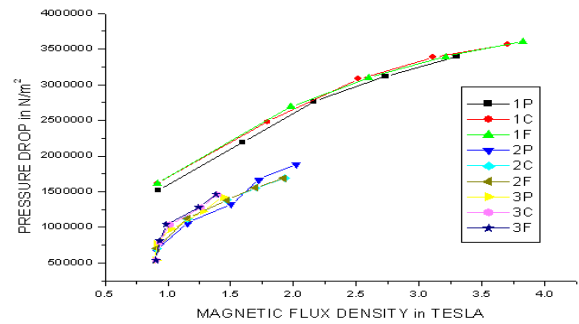


Fig 26 c. Variation of Pressure drop with Magnetic Flux Density for a Piston Velocity of 0.12m/s

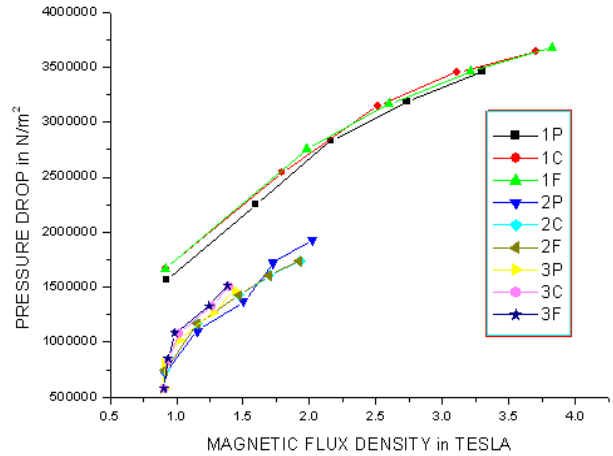


Fig 26 d. Variation of Pressure drop with Magnetic Flux Density for a Piston Velocity of 0.16 m/s

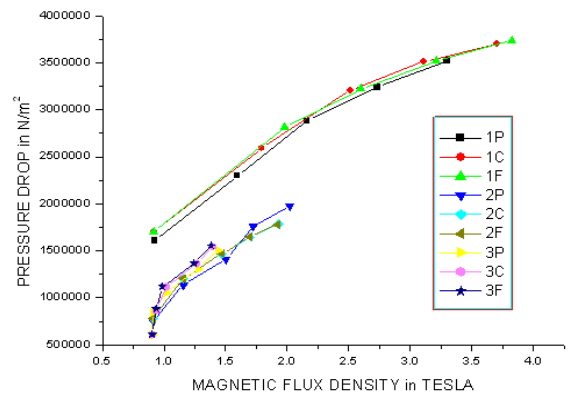


Fig 26e. Variation of Pressure drop with Magnetic Flux Density for a Piston Velocity of 0.2 m/s

The simulation results of pressure drop with respect to flow rate for a variation in current from 0.4 amp to 2 amp and constant gap of 0.4 mm for various models are shown in fig 14a to 14e.

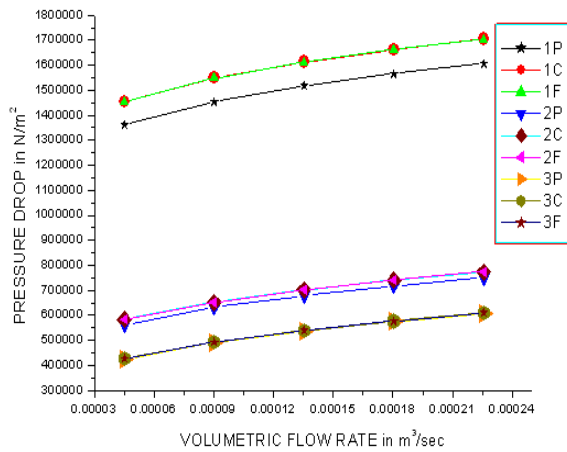


Fig 27a. Variation of Pressure drop with Volumetric Flow Rate for a Current of 0.4 A

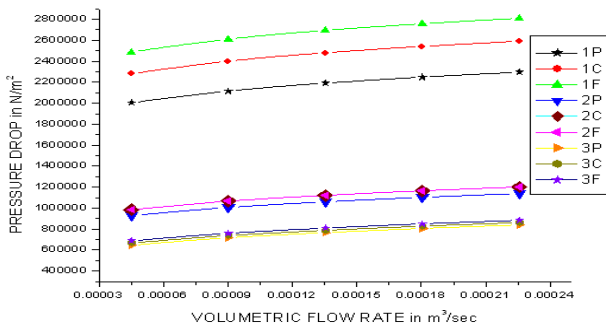


Fig 27b. Variation of Pressure drop with Volumetric Flow Rate for a Current of 0.8 A

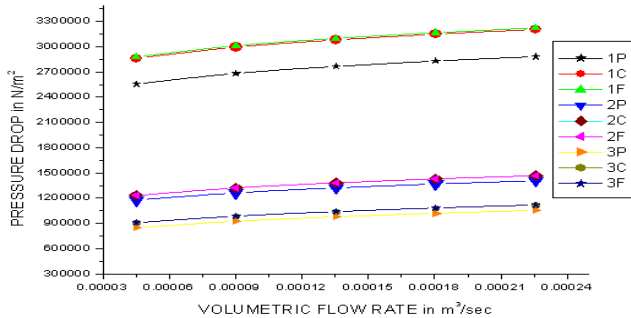


Fig 27c. Variation of Pressure drop with Volumetric Flow Rate for a Current of 1.2 A

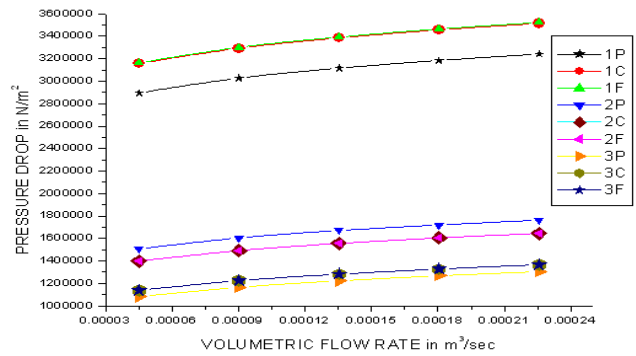


Fig 27d. Variation of Pressure drop with Volumetric Flow Rate for a Current of 1.6 A

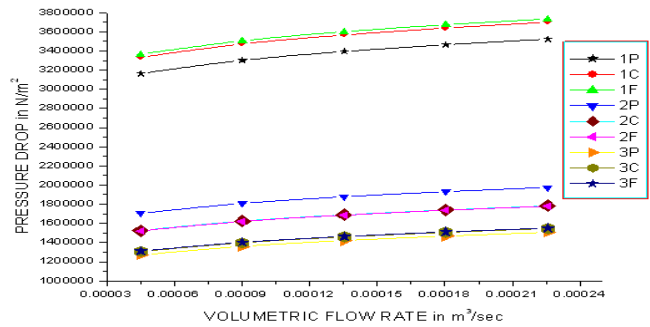


Fig 27e. Variation of Pressure drop with Volumetric Flow Rate for a Current of 2 A

It is observed from Fig. 13a to Fig.13e that as current increases, the magnetic flux density also increases which results in an increase in pressure drop. For a given current, the pressure drop increases with increase in velocity. This trend is observed for currents up to 1.6A. However at 2A current the pressure drop is less at lower velocities but it gradually increases at higher velocities to reach a maximum. Maximum pressure drop is observed in case of single stage with filleted piston end model. The figures from 14a to 14e show that the pressure drop increases with increase in flow rate of MR fluid. The maximum pressure drop with respect to flow rate is also found to occur in case of one stage model with filleted piston ends

VI. CONCLUSION

In the present paper, the performances of an MR fluid damper with nine different configurations are studied. It can be concluded from the evaluation of the above models that, the model with filleted ends gives optimum pressure drop with respect to magnetic flux density as well as flow rate. This implies that higher loads can be carried by the damper even with small capacities.

Analysis of Magneto Rheological Fluid Damper with Various Piston Profiles

REFERENCES

- [1] Hiroshi Sodeyama, Kohei Suzuki, Katsuaki Sunakoda "Development of Large Capacity semi- active Seismic damper using Magneto – Rheological Fluid", Journal of Pressure Vessel Technology, Vol. 126 ,pp 105-109, Feb 2004
- [2] Maher Yahya Salloom & Zahurin Samad "Finite element modeling and simulation of proposed design magneto-rheological valve" International Journal advanced manufacturing Technology, Vol 54 numbers 5-8, pp421 – 429, May 2011
- [3] H.yoshioka, J.C. Ramallo, B.F. Spencer et al; "Smart Base Isolation strategies Employing Magnetorheological Dampers" Journal of engineering mechanics, pp 540-551 May 2002
- [4] Laura M, Jansen and Shirley J. Dyke "Semi active control strategies for MR Dampers Comparative Study "Journal of Engineering Mechanics, Vol. 126, No. 8, pp795-803, August 2000
- [5] B.F. Spencer Jr., S.J. Dyke, M.K. Sain and J. D. Carlson "Phenomenological Model for Magnetorheological Damper" Journal of engineering mechanics Vol.123, No. 3, pp230-238, March, 1997
- [6] N.Seetharamaiah, Sadak Ali Khan and K.Narayanarao, "Design of Small Capacity MR Fluid Damper" International Journal on Mechanical and Automobile Engineering Vol. 01, NO.1 , Nov. 2008-, 29-36, pp29-36, Jan 2009
- [7] Chun-Yu lai and W.H. Liao "Vibration Control of a Suspension system via Magneto rheological Fluid Damper" Journal of Vibration and Control, Vol 8, pp527-547, 2002
- [8] Butz.T and Von Stryk.O "Modelling and simulation of Electro and Magnetorheological fluid dampers", zamm, Vol. 82, No. 1, pp. 3-20, 2002
- [9] Laura M, Jansen and Shirley J. Dyke "Semi Active Control Strategies for MR Dampers: Comparative study", Journal of engineering mechanics, Vol.126 No.8, pp 795-803, Aug 2000
- [10] Henri GAVIN, Jesse HOAGG and Mark DOBOSSY "Optimal Design of MR Dampers" Smart structures for improved Seismic performance, pp225-236, Aug 2001